Published April 1, 1993

Clathrin and HA2 Adaptors: Effects of Potassium Depletion, Hypertonic Medium, and Cytosol Acidification

Steen H. Hansen, Kirsten Sandvig,* and Bo van Deurs

Structural Cell Biology Unit, Department of Anatomy, The Panum Institute, University of Copenhagen, DK-2200 Copenhagen N, Denmark; and *Institute for Cancer Research at the Norwegian Radium Hospital, Montebello, 0310 Oslo 3, Norway

Abstract. The effects of methods known to perturb endocytosis from clathrin-coated pits on the localization of clathrin and HA2 adaptors in HEp-2 carcinoma cells have been studied by immunofluorescence and ultrastructural immunogold microscopy, using internalization of transferrin as a functional assay. Potassium depletion, as well as incubation in hypertonic medium, remove membrane-associated clathrin lattices: flat clathrin lattices and coated pits from the plasma membrane, and clathrin-coated vesicles from the cytoplasm, as well as those budding from the TGN. In contrast, immunofluorescence microscopy using antibodies specific for the α- and β-adaptins, respectively, and immunogold labeling of cryosections with anti-α-adaptin antibodies shows that under these conditions HA2 adaptors are aggregated at the plasma membrane to the same extent as in control cells. After reconstitution with isotonic K^+-containing medium, adaptor aggregates and clathrin lattices colocalize at the plasma membrane as normally and internalization of transferrin resumes. Acidification of the cytosol affects neither clathrin nor HA2 adaptors as studied by immunofluorescence microscopy. However, quantitative ultrastructural observations reveal that acidification of the cytosol results in formation of heterogeneously sized and in average smaller clathrin-coated pits at the plasma membrane and buds on the TGN. Collectively, our observations indicate that the methods to perturb formation of clathrin-coated vesicles act by different mechanisms: acidification of the cytosol by affecting clathrin-coated membrane domains in a way that interferes with budding of clathrin-coated vesicles from the plasma membrane as well as from the TGN; potassium depletion and incubation in hypertonic medium by preventing clathrin and adaptors from interacting. Furthermore our observations show that adaptor aggregates can exist at the plasma membrane independent of clathrin lattices and raise the possibility that adaptor aggregates can form nucleation sites for clathrin lattices.

CLATHRIN and adaptors of the HA2 type provide the molecular apparatus for selective and efficient internalization of transmembrane proteins containing a recognition sequence for coated pits in their cytoplasmic tail (4, 23, 33, 37, 40, 45, 51, 53).

Part of the information on the role of clathrin-coated pits in endocytosis has been generated by treatments that perturb endocytosis from clathrin-coated pits in intact cells, such as K^+ depletion, incubation in hypertonic medium, and cytosol acidification. Larkin et al. (24–26) showed that depleting fibroblasts as well as hepatocytes of K^+ resulted in disappearance of clathrin-coated pits from the plasma membrane as revealed by EM and caused a marked reduction in the rate of endocytosis of receptor-bound LDL. Daukas and Zigmond (9) observed that incubating polymorphonuclear leukocytes in hypertonic medium had little effect on receptor binding, but inhibited receptor-mediated uptake of the chemotactic peptide f-NleLeuPhe. Subsequently, Oka et al. (36), studying the internalization of asialo-orosomucoid by the galactosyl receptor system in rat hepatocytes, showed that hypertonic medium caused a disappearance of coated pits similar to the effect of K^+ depletion. Sandvig et al. (44) found that acidification of the cytosol of several cell types perturbed endocytosis of transferrin and EGF by inhibiting invaginated coated pits from pinching off. Thus, coated pits still contained transferrin receptors and occurred with normal frequency in acidified cells (44). Also, Davoust et al. (11) found that acidification of the cytosol reduces uptake of HRP.

K^+ depletion, incubation in hypertonic medium, and cytosol acidification have been used to study the dynamic interactions between transmembrane proteins and coated pits using fluorescence photobleaching recovery (13), to document the clathrin-mediated entry of transmembrane proteins including receptors with mutated internalization signals (2, 13, 15, 22, 31), as well as toxins (34, 41, 43) and viruses (28), and to study the secretory pathway (8, 12). These

Dr. Hansen's present address is Johns Hopkins University, Department of Biology, 144 Mudd Hall/3400 N. Charles Street, Baltimore, MD 21218.

Published April 1, 1993

methods have also provided the bulk of data on clathrin-independent endocytic mechanisms (9, 17, 28, 34–36, 41–44, 52, 55, 56).

The effects of K^+ depletion, and incubation in hypertonic medium on membrane-associated clathrin lattices in replicas of the inner surface of plasma membranes of freeze-etched fibroblasts have been studied in great detail by Heuser and Anderson (20). After both K^+ depletion and incubation in hypertonic medium, coated pits were found to be replaced by accumulations of microcages: small round (50–70-nm diam) geodesic clathrin lattices devoid of internal membrane (empty cages) (20). Numerous microcages were also detected in an accompanying study of acidified cells, in this case associated with deeply invaginated (paralyzed) coated pits (19). Based on these data, it was suggested that K^+ depletion and incubation in hypertonic medium both perturb endocytosis from coated pits by trapping clathrin in microcages (20), and that cytosol acidification has a similar effect (19).

However, ultrastructural immunocytochemical data on the cellular distribution of clathrin following any of these perturbations have to our knowledge not been published and the effects on adaptor molecules have not been reported. Moreover, it has been known for a long time that clathrin-coated vesicles formed at the plasma membrane are differently sized from those formed at the Golgi complex (14). It is not clear whether clathrin-coated domains at these two locations react in the same way after potassium depletion, incubation in hypertonic medium, and cytosol acidification. These issues are important in view of the data previously obtained and of the continuous use of all three methods and have therefore been addressed in the present work using fluorescence microscopy and ultrastructural immunocytochemistry.

We show that in HEp-2 cells, K^+ depletion in combination with a hypotonic shock, as well as incubation in hypertonic medium (0.45 M sucrose), removes membrane-associated clathrin lattices and thus results in disappearance of clathrin-coated vesicles, plasma membrane coated pits and clathrin-coated buds on the TGN. In contrast, acidification of the cytosol paralyzes clathrin in the membrane-bound state, leading to formation of smaller and more heterogeneously sized coated pits at the plasma membrane and buds at the TGN. Yet, under all three conditions where endocytosis of transferrin is arrested, HA-2 adaptors occur in aggregates of the same size and frequency as found in control cells. Transfer of HEp-2 cells perturbed by K^+ depletion or hypertonicity to isotonic K^+-containing medium results in reconstitution of clathrin-coated membrane domains including coated pits, suggesting that pre-existing adaptor aggregates can serve as nucleation sites. The coated pits in reconstituted cells are "functional," since they pinch off to form coated vesicles delivering transferrin to endosomes.

Materials and Methods

K^+ Depletion, Incubation in Hypertonic Medium, and Acidification of the Cytosol

HEp-2 cells were grown as previously described (17) and processed for K^+ depletion (24), incubation in hypertonic medium (9), and acidification of the cytosol (44) as outlined in Fig. 1. The buffer used for potassium depletion contained 0.14 M NaCl, 20 mM Hepes, 1 mM $CaCl_2$, 1 mM $MgCl_2$, and 1 g/l D-glucose. Control cultures were incubated in the same buffer supplemented with 10 mM KCl. Hypertonic medium consisted of DME-H (DME containing 2 mM L-glutamine and 20 mM Hepes, without sodium bicarbonate; Flow Laboratories, Irvine, Scotland) supplemented with 0.45 M sucrose. For acidification of the cytosol, 1 M acetic acid, pH 5.0 (NaOH), was added 1:100 to DME-H, pH 5.0 (HCl), whereas controls were incubated in DME-H, pH 5.0.

Transferrin Uptake Assays

Iron-saturation of transferrin was carried out according to Dautry-Varsat (10). For biochemical measurements, endocytosis of ^{125}I-labeled transferrin–128 ng/ml; 27 cpm/pg–was determined as described by Ciechanover et al. (7). In experiments for fluorescence microscopy, perturbed, and control cultures of HEp-2 cells were transferred to ice, rinsed in ice-cold K^+-supplemented or K^+-free medium and incubated with either 50 μg/ml unlabeled transferrin or 50 μg/ml transferrin-Texas red (Molecular Probes Inc., Eugene, OR) for 20 min on ice followed by 20 min at 37°C in prewarmed but otherwise identical medium. No difference in the results obtained with transferrin–Texas red and native transferrin detected by immunofluorescence were recorded. In some experiments, transferrin was omitted to ascertain the specificity of the subsequent immunolabeling. To remove surface-bound transferrin, cells were either treated with pronase (7), or acid treated according to Stoppelli et al. (48), except that all procedures were carried out on ice.

Immunofluorescence Microscopy

Antibodies. Clathrin was detected using 2 μg/ml mouse monoclonal IgM anti-clathrin antibody, clone C_{HC} 5.9 (5) (Boehringer-Mannheim GmbH, Mannheim, Germany) followed by Texas red–conjugated goat anti-mouse IgM (Southern Biotech, Birmingham, AL; code no. 1020-07) diluted 1:20 or fluorescein-conjugated goat anti-mouse IgM (Medac, Hamburg, Germany; code no. 31501) diluted 1:100.

HA2 adaptor protein was detected with mouse monoclonal anti-α-adaptin antibodies, AC1-M11 (IgG2a) (39), and AP-6 (IgG1) (6) as well as mAb 100/1 (IgG1) (1) against β- and β′-adaptin, followed either by rhodamine-conjugated goat anti-mouse IgG (Tago Inc., Burlingame CA; code no. 6350) and rhodamine-conjugated mouse anti-goat IgG (Accurate Chem. & Sci. Corp., Westbury, NY; code no. JMG-025-108) both diluted 1:25, or by Texas red–conjugated goat anti-mouse IgG1/IgG2a (Southern Biotech; code no. 1070-07/1080-07) diluted 1:30.

Transferrin was detected with rabbit anti-transferrin antiserum (DAKO-PATTS, Copenhagen, Denmark; code no. A061) followed by fluorescein-conjugated goat anti-rabbit IgG (Southern Biotech; code no. 4030-02) both diluted 1:20.

Fixation/Permeabilization. Three protocols were used for fixation and permeabilization: (*a*) Fixation/permabilization with methanol 5 min at −20°C; (*b*) fixation with 2% paraformaldehyde in 0.1 M phosphate buffer, pH 7.2, 5 min at 4°C followed by rinsing twice in PBS and permeabilization with methanol for 90 s at 4°C; and (*c*) fixation with 2% paraformaldehyde in 0.1 M phosphate buffer, pH 7.2, 5 min at 4°C followed by rinsing twice in PBS and permeabilization with 0.5% Triton X-100 for 5 min at room temperature. Experiments involving antibodies specific for clathrin and/or transferrin were performed with protocols *a* and *b* and essentially identical results were obtained. AC1-M11 requires denaturation of antigen, and thus protocol *a*. mAb 100/1 works best with protocol a (1). Protocol *c* was used for AP-6 since it does not resist methanol. In contrast, CHC 5.9 seemed to require methanol to resist detergents and double labeling experiments were therefore performed in conjunction with AC1-M11.

Immunocytochemistry. All procedures were carried out at room temperature. Fixed and permeabilized specimens of sparse–20% confluent–HEp-2 cultures were rinsed with PBS (without calcium and magnesium), the T-25 flasks cut open and 1-cm^2 incubation fields framed by wiping the surrounding cells off. The fields were then incubated in PBS containing 10% normal goat serum and 0.1% saponin (PBS-NGS)[1] for 10 min followed by incubation for 30 min each with primary and secondary antibodies diluted in PBS-NGS with three rinses in PBS after each antibody incubation. For single labeling of HA-2 adaptors, an extra layer of fluorescent antibody was used in some experiments to intensify the signal, and in this case 1% BSA and 0.2% gelatin was substituted for normal goat serum in the incubation buffer.

In double-labeling experiments, incubation with primary and secondary

1. *Abbreviation used in this paper*: NGS, normal goat serum.

Published April 1, 1993

antibodies respectively was carried out simultaneously, and secondary antibodies were selected on the basis of their lack of reactivity in controls comprising (*a*) exclusion of either anti-clathrin or anti-adaptin antibody alone or (*b*) in combination with exclusion of secondary antibody specific for the primary antibody present during the primary antibody incubation.

Finally, specimens were air-dried, mounted in Fluoromount G containing 2.5 mg/ml *n*-propyl gallate, examined in a microscope (Ernst Leitz Wetzlar GMBH, Germany) equipped with epifluorescence optics, and photographed using a 63× oil-immersion objective.

Immunolabeling of Cryosections to Detect Clathrin

The protocol for the Tokuyasu technique (49) was based on modifications devised by Griffiths et al. (16), Tokuyasu (50), and Slot et al. (46).

Preparation of Cryosections. 80% confluent cultures were processed for potassium depletion according to the protocol shown in Fig. 1 and fixed in 8% paraformaldehyde in 0.15 M Hepes pH 7.5 for 2 h at room temperature followed by 20 h at 4°C. The cells were then scraped off, pelleted by centrifugation (500 *g* for 5 min), resuspended in PBS containing 10% gelatin at 37°C, pelleted again (1,000 *g* for 5 min), and then placed on ice for 15 min for the gelatin to solidify. The pellets were then cut out, transferred to 2.3 M sucrose in PBS on ice, cut into 1-mm^3 blocks, infiltrated with 2.3 M sucrose in PBS overnight at 4°C, mounted (on ice) on stubs, frozen in liquid nitrogen, and sectioned on an LKB Ultratome CryoNova or a RMC MT-7.

Immunolabeling. Grids were at room temperature incubated for 30 min on puddles of PBS containing 10% FCS and 0.02 M glycine (PBS-FCS) followed by incubation for 30 min with anti-clathrin antibody clone C_{HC} 5.9, 2 μg/ml in PBS-FCS, and rinsed for 5 min ×6 in PBS-FCS. Next, sections were incubated with goat anti-mouse IgM coupled to 10 nm colloidal gold (Amersham International, Amersham, UK; code no. RPN 428) diluted 1:10 in PBS-FCS, and rinsed for 5 min ×6 in PBS-FCS, followed by PBS ×4, and distilled water ×4. Finally, sections were contrasted/embedded in 2% methyl cellulose containing 0.3% uranyl acetate for 7 min on ice, air-dried, and examined in a JEOL 100CX microscope.

Microscopy of ultrathin cryosections of HEp-2 cells incubated with the anti-clathrin antibody clone C_{HC} 5.9 revealed cross-reactivity to a component in the nucleolus. This labeling showed the same sensitivity to dilution as the reaction with clathrin-coated pits, and could not be blocked by a 100-fold excess of human IgM (which is not detected by the secondary antibody). Substitution of fixative (with 2% paraformaldehyde, 0.1% glutaraldehyde in 0.1 M phosphate buffer, pH 7.2), cryoprotectant (with PVP-sucrose), incubation buffer (with BSA/gelatin), and increasing glycine concentration (to 0.2 M before or during incubation with PBS-FCS) also had no effect. No further reference to the cross-reaction is made, however, since it has no relevance to the data reported in the Results section.

Immunolabeling of Cryosections to Detect AP-6

Attempts to detect HA2 adaptors in ultrathin sections using the protocols described for clathrin above resulted in very low labeling when using AP-6 and no reactivity with mAb 100/1. Using AP-6, Hille et al. (21) detected HA2 adaptors in cryosections of BHK cells fixed in 2% paraformaldehyde in PBS. With this fixative we obtained increased labeling of HA-2 adaptors in HEp-2 cells but the efficiency in percent labeled coated pits still remained low and was approximately equal with each of the six different detection systems tested comprising two rabbit anti-mouse antibodies and protein A coupled to 5 or 10 nm colloidal gold and goat anti-mouse IgG coupled to 5 or 10 nm gold.

Quantification of Relative Surface Areas of Clathrin-coated Domains of the Plasma Membrane and TGN in Control and Acidified Cells. Micrographs (primary magnification of 23,700) of clathrin-coated domains (plasma membrane and TGN) in acidified and control cells from random cryosections—of appropriate thickness and preservation—were printed at final magnification of 66,360× and overlaid with a single-lattice grid type A100 (54) with grid-size 2.5 mm (38 nm) to determine the number of intersections with clathrin-coated domains. The plasma membrane population was identified either as pits in direct (visible) continuity with plasma membrane or as clathrin-coated profiles within three vesicle diameters from the plasma membrane (38). The TGN population was defined similarly. Equivocal clathrin-coated profiles were excluded. The quantification was continued until approximately 250 intersections in each of the four categories were obtained (reached after 18 and 25 micrographs from acidified and control cells, respectively). Statistics were performed as previously described (18).

Results

Fate of Clathrin as Revealed by Fluorescence Microscopy

The experimental protocols used for acidification of the cytosol, K^+-depletion, and incubation of HEp-2 cells in hypertonic medium are outlined in Fig. 1.

Using anti-clathrin heavy chain C_{HC} 5.9, the presence of clathrin-coated pits and vesicles in control cells was revealed by immunofluorescence as distinctly punctate (Fig. 2, *A* and *A'*). The minute fluorescent dots sometimes formed short rows, presumably reflecting the alignment of clathrin-coated pits between stress fibers just below the plasma membrane (26). Internalization of transferrin was used as functional assay to assess the receptor-mediated endocytosis from coated pits. In control cells, transferrin-containing endosomes gave a dotted fluorescence (Fig. 2 *B*).

In contrast, after incubation in hypertonic medium (Fig. 2 *C*) as well as after K^+ depletion (data not shown), the labeling specific for clathrin changed to a fuzzy granular image, in agreement with previous reports (19, 24, 26). Concomitantly, there was no fluorescence specific for transferrin in more than 90% of the cells and a reduced uptake in the remaining cells after incubation in hypertonic medium (Fig. 2 *D*) or K^+ depletion (data not shown), clearly demonstrating that transferrin uptake was efficiently arrested by these experimental treatments. Biochemical measurements of ^{125}I-transferrin uptake using the same protocols for perturbing clathrin function showed—in agreement with the fluorescence observations—that endocytosis of transferrin was strongly reduced (Fig. 3).

Acidification of the cytosol also inhibited the uptake of transferrin as measured biochemically and by immunofluorescence microscopy. However, in contrast to the effect of K^+ depletion and incubation in hypertonic medium, acidification did not change the distinct punctate fluorescence pattern specific for clathrin (data not shown).

Fate of Clathrin as Revealed by EM

To further characterize the effects of the methods studied to perturb endocytosis from coated pits on the distribution of

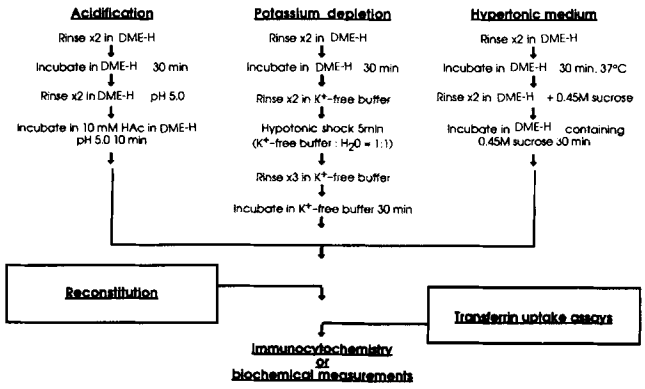

Figure 1. Flow chart outlining the protocols to process HEp-2 cells for acidification of the cytosol using acetic acid, for K^+ depletion in combination with a hypotonic shock, and for incubation in hypertonic medium. DME-H: DME containing 2 mM L-glutamine and 20 mM Hepes, without sodium bicarbonate.

Published April 1, 1993

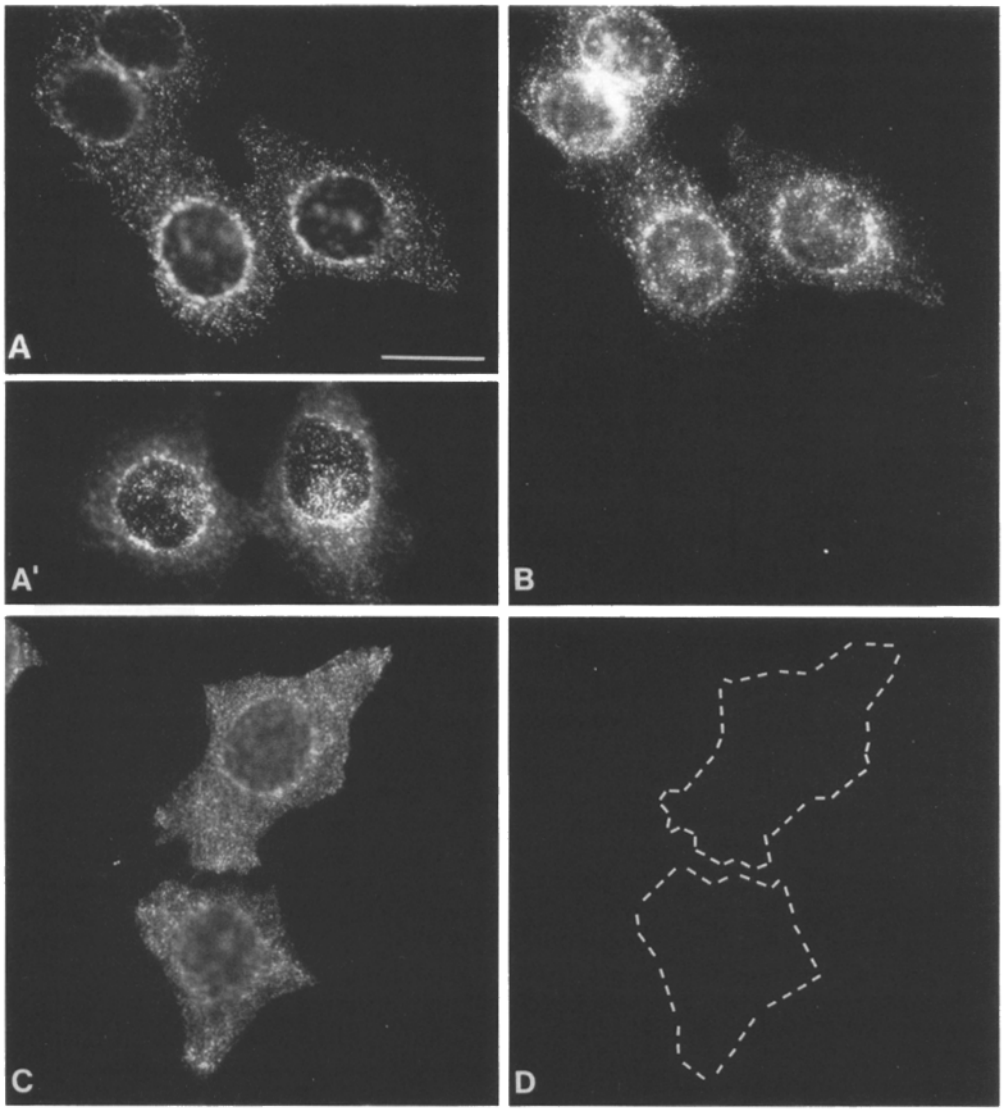

Figure 2. Effect of hypertonic medium on endocytosis of transferrin-Texas red and immunolocalization of clathrin by double-labeling fluorescence microscopy. HEp-2 cells were incubated at 37°C for 30 min in DME-H followed by additional 30 min in DME-H (*A* and *B*) or DME-H + 0.45 M sucrose (*C* and *D*), and then incubated for 20 min in the same media containing 50 μg/ml transferrin-Texas red. The cells were then chilled to 4°C and surface-bound transferrin-Texas red was removed by acid treatment. After fixation, the cells were processed for immunolocalization of clathrin as described in Materials and Methods using anti-clathrin heavy chain IgM C_{HC} 5.9 followed by fluorescein-labeled goat anti-mouse IgM antibody. (*A* and *C*) fluorescein filter. (*B* and *D*) Texas red-filter. Note that the fluffy fluorescence in the nuclei of control cells immunolabeled to localize clathrin (*A*) is due to distinct punctate fluorescence from coated pits above the nuclei that are out of focus (*A'*). Due to fading of fluorescein, it was not possible to illustrate this point for the same cells as shown in *A*. Bar, 10 μm.

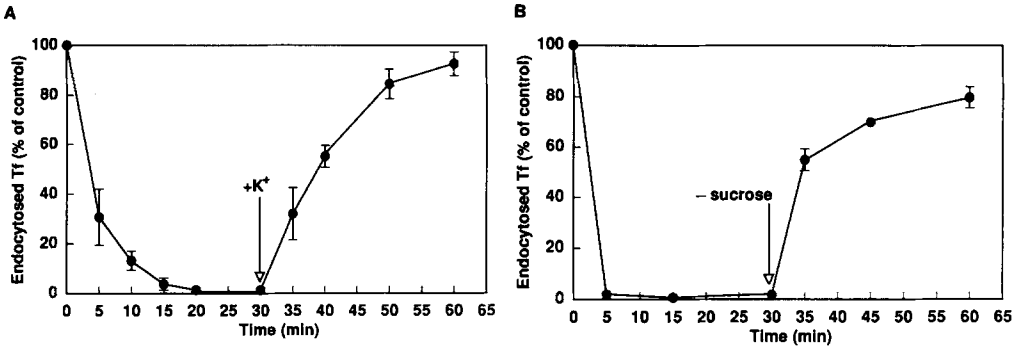

Figure 3. Transferrin endocytosis in K^+-depleted (*A*), and hypertonically treated cells (*B*) in percent of respective controls. For K^+ depletion (*A*), HEp-2 cells growing in 4-well disposable trays were subjected to a hypotonic shock in the absence of potassium as described in Materials and Methods and as summarized in Fig. 1. The cells were then transferred to K^+-free buffer, and ^{125}I-labeled transferrin was added after different periods of time. 5 min after addition of transferrin, the amounts of bound and endocytosed transferrin were measured as described in Materials and Methods. Next, DME-H was added to cells which had been incubated in the absence of K^+ for 30 min, and again endocytosis of transferrin was measured after different periods of time. In each experiment, transferrin endocytosis was also measured in parallel cultures which had been hypotonically shocked but not K^+ depleted (control). The results shown are the mean values from two to four different experiments. The bars show the range of variation between experiments. Non-specific binding was estimated as pronase-resistant radioactivity in parallels incubated with ^{125}I-transferrin at 4°C and subtracted. Note that time points are placed in the middle of the period of incubation with ^{125}I-transferrin. For instance, the 2.5-min value shows transferrin endocytosis in K^+-depleted cells in percentage of the control within the first 5 min after the hypotonic shock. (*B*) Hypertonically treated cells (DME-H + 0.45 M sucrose) and control cultures (DME-H only) were processed for determination of transferrin endocytosis accordingly.

Published April 1, 1993

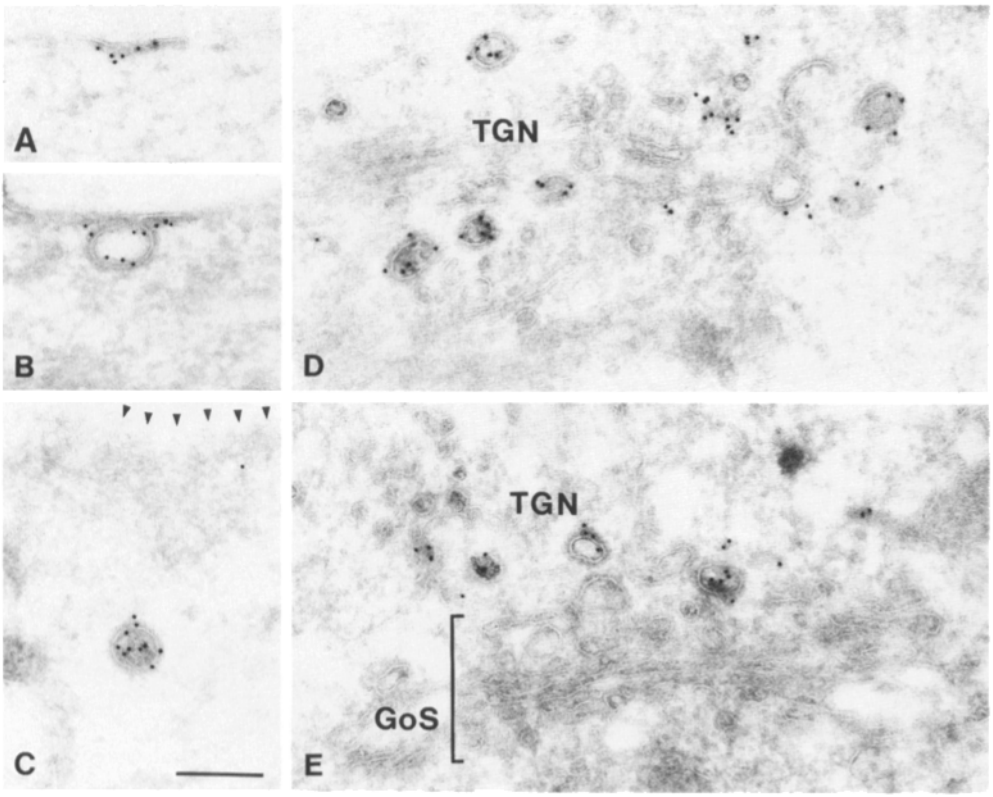

Figure 4. Localization of clathrin in cryosections of control HEp-2 cells labeled with anti-clathrin antibody C_{HC} 5.9 (IgM) followed by goat anti-mouse IgM coupled to 10 nm colloidal gold to show the reactivity of C_{HC} 5.9 with flat clathrin-coated membrane domains (*A*), coated pits (*B*) and presumptive vesicles (*C*), and clathrin-coated vesicles budding from the TGN (*D* and *E*). The tangentially cut plasma membrane in *C* is indicated by arrowheads. (*A–C*) Hypotonically shocked HEp-2 cells incubated in K^+-supplemented medium. (*D* and *E*) HEp-2 cells incubated in DME-H. *GoS*, Golgi stack. Bar, 200 nm.

clathrin, we labeled ultrathin cryosections of control and experimentally processed cells with anti-clathrin C_{HC} 5.9. In addition to some scattered cytoplasmic labeling, profiles of control cells exhibited rare, flat clathrin-coated membrane domains, numerous clathrin-coated pits and vesicles, as well as clathrin-coated buds on the *trans*-Golgi network (Fig. 4). Only sparse labeling of membrane not visibly coated was observed.

In agreement with previous studies (17, 20, 24–26, 28) we found that K^+ depletion and incubation in hypertonic medium remove clathrin-coated pits from the plasma membrane. We furthermore found that clathrin-coated membrane domains were absent from the cytoplasm, showing that the clathrin of free clathrin-coated vesicles and clathrin-coated vesicles budding from the TGN also is removed by these treatments. In fact, in six independent experiments where HEp-2 cells from different passages were K^+ depleted (Fig. 5) or hypertonically treated (data not shown), followed by processing for immunogold labeling of cryosections, we detected little membrane-associated clathrin altogether. Instead we repeatedly found that the level of cytoplasmic labeling increased (Fig. 5). The sparse residual gold particles occurring at membranes were scattered, and not associated with coat material and therefore most likely reflected either clathrin in the neighboring cytoplasm, or clathrin adhering non-specifically to membranes.

Essentially the same structures that were labeled in controls were also tagged by gold particles in acidified cells, although some modifications were noticed (Fig. 6). First, plasma membrane–coated pits tended to form clusters. Second, although not frequently encountered (roughly one out of ten cell profiles), additional labeling of plasma membrane domains was observed. Characteristically the membrane at these sites was cut tangentially and the gold particles were typically separated from the outer cell limit by 30–60 nm. These domains most likely correspond to the edges of clusters of coated pits that were hit peripherally in the section. Third, clathrin-coated pits were more heterogeneously sized due to the occurrence of unusually small pits. Also, clathrin-coated buds on the TGN were reduced in size in acidified cells. To obtain quantitative data and circumvent problems with the many different conformations adopted by clathrin-coated domains, we determined the number of intersections of clathrin-coated domains of the plasma membrane and TGN with a single lattice grid as described in Materials and Methods as a relative measure of their size in acidified cells and controls. As shown in Table I, acidification of the cytosol leads to a significant decrease in surface area of both plasma membrane and TGN populations of clathrin-coated domains with concomitant increase in heterogeneity revealed by >100 and 60% increase in coefficients of variation for the plasma membrane and TGN population, respectively (Table I). These differences were not simply due to different labeling efficiencies in acidified cells and controls. The number of gold particles per intersection with coated domains was essentially identical in all four situations (Table I). It should be noticed that the ratio between the size of the plasma membrane and TGN populations of clathrin-coated membrane domains were maintained after cytosol acidification; 1.6 (12.35/7.79) and 1.5 (8.22/5.67) in control and acidified cells, respectively (Table I).

It would seem obvious also to quantify the relative amounts of clathrin associated with various membrane domains and with the cytoplasm, respectively, under the different experimental conditions studied. However, during the course of this work, several problems were encountered which in our

Published April 1, 1993

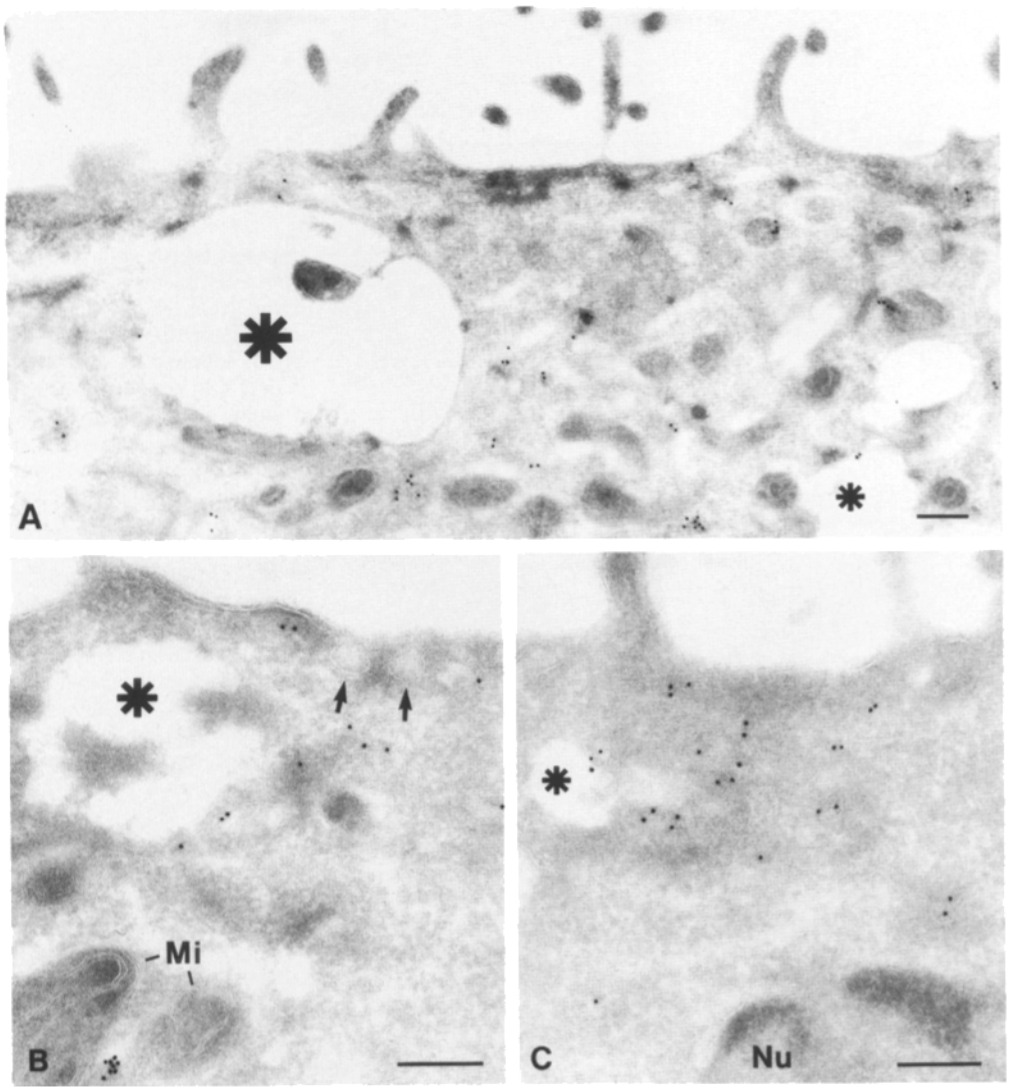

Figure 5. Localization of clathrin in cryosections of K^+-depleted HEp-2 cells labeled to detect clathrin as in Fig. 4. (*Nu*) nucleus; (*Mi*) mitochondria; (*) cytoplasmic puffs characteristically found in K^+-depleted cells (see reference 28); arrows, plasma membrane pits without clathrin coats. The clathrin appears scattered throughout the cytoplasm. Bar, 200 nm.

opinion would make such quantitative data unreliable. First, it was noted that the labeling efficiency of anti-clathrin CHC 5.9 increased with decreasing section thickness, thus requiring sections of thickness within a narrow range to obtain optimal results and comparable conditions. In contrast to the situation with clathrin-coated membrane domains, there is no "internal control" in the case of cytoplasmic clathrin. Second, in these rather thin sections, cytoplasmic clathrin may well be extracted, and the extent to which this occurs may depend upon the experimental condition studied. Third, it is difficult, especially using a mAb, to obtain a reliable estimate of the level of background labeling in the cytoplasm. Omission of the primary antibody evidently results in an unrealistic low level of nonspecific labeling. On the other hand, attempts to use a monoclonal non-sense IgM to estimate non-specific binding also failed, since it decorated the cells massively with gold.

Fate of Adaptors as Revealed by Fluorescence Microscopy

Using the mAbs AC1 M11 (39) and AP-6 (6) against both α-adaptins found in the HA2 adaptor, immunofluorescence microscopy of control cells revealed a distinct, punctate pattern (Fig. 7) corresponding to the appearance of plasma membrane clathrin lattices. Both the size and frequency of α-adaptin aggregates were thus the same as found for clathrin. Some perinuclear staining was also noted. This is most likely due to poor resolution of adaptor aggregates in the membrane on the sides of the bulging nucleus, since most of the perinuclear staining obtained on formalin-fixed cells (AP-6) could be resolved as individual dots by focusing. It could also result from a cytoplasmic pool of α-adaptins. As expected, the localization by immunofluorescence of α-adaptins in acidified cells did not deviate from controls (data not shown). Interestingly, however, K^+ depletion and incubation in hypertonic medium also did not change the distribution of α-adaptins (Fig. 7). Using mAb 100/1 specific for the β- and β'-adaptins of the plasma membrane and the Golgi adaptor, respectively (1), and focusing on cell processes assumed to be devoid of TGN components, we also found β-adaptin aggregates at the plasma membrane in K^+ depleted and hypertonically treated cells similar to controls (data not shown).

Fate of Adaptors as Revealed by EM

Ultrastructural observations obtained with AP-6 showed

Published April 1, 1993

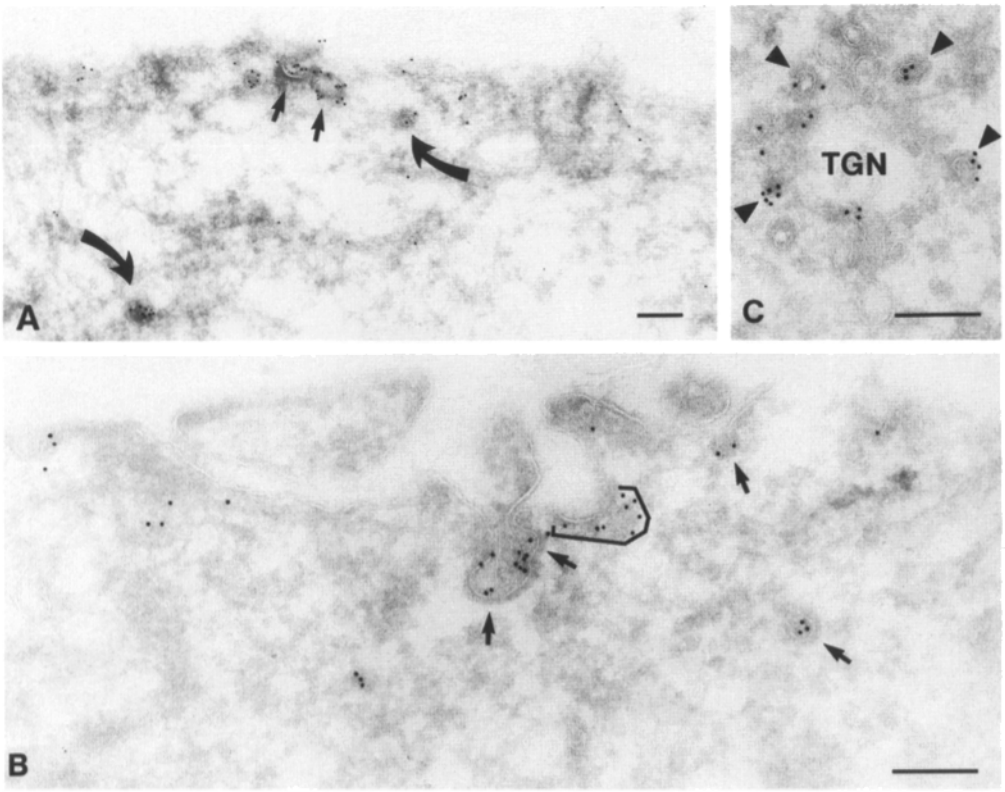

Figure 6. Localization of clathrin in cryosections of acidified HEp-2 cells labeled to detect clathrin as in Fig. 4. (*A* and *B*) Note the clusters and heterogeneous size of coated pits (*small arrows*), and the presence of apparently free clathrin-coated vesicles (*curved arrows*). The bracket in *B* indicates a cluster of coated pits hit tangentially. (*C*) Arrowheads indicate clathrin-coated buds on the TGN labeled by the antibody. Bar, 200 nm.

labeling of flat and invaginated coated membrane domains and coated vesicles (Fig. 8) and furthermore confirmed the presence of α-adaptins at the plasma membrane following K^+ depletion or incubation in hypertonic medium (Fig. 8). In the K^+-depleted and hypertonically treated cells, most of the plasma membrane-associated labeling was found at flat domains (Fig. 8). Invaginated plasma membrane domains were occasionally tagged but these could be remnants of coated pits (not shown). However, it should be stressed that the labeling with AP-6 was low. In 25 systematically sampled profiles of control cells from a section considered optimally labeled using goat anti-mouse IgG coupled to 10 nm gold, we observed 107 coated pits containing 91 (62%) out of a total of 147 plasma membrane associated gold particles representing fewer antigenic sites due to empty amplification (47). Of these 107 coated pits, 51% were not labeled, 26, 15, 7, and 2% were tagged by 1, 2, 3, and >3 gold particles, respectively. Attempts to double-label ultrathin cryosections convincingly for clathrin and HA2 adaptors were unsuccessful as a result of inadequate labeling with AP-6. Thus, although AP-6 clearly gave specific reactions, the low labeling on cryosections posed severe restrictions on its use for EM in the present study and the data obtained for adaptors therefore relies mainly on immunofluorescence.

Collectively these data show that intact HA2 adaptors are aggregated at the plasma membrane of HEp-2 cells after clathrin lattices have been removed by K^+ depletion or incubation in hypertonic medium.

Table I. Effect of Cytosol Acidification on Clathrin-coated Domains of the Plasma Membrane (PM) and TGN

Membrane	Treatment	ΣIntersection	ΣCoated domains	Intersection/coated domains	*t* test: control vs. acidified P value	Intersection/coated domain Coefficient of variation	Gold particles/intersection coated domain
				(*Mean* ± *SEM*)		(%)	(*Mean* ± *SEM*)**
PM							
	Control	247	20	12.35 ± 0.66§		23.8	0.58 ± 0.07
					<0.01*		
	Acidified	263	32	8.22 ± 0.83‖		56.8	0.59 ± 0.06
TGN							
	Control	257	33	7.79 ± 0.31§		23.1	0.65 ± 0.06
					<0.001‡		
	Acidified	255	45	5.67 ± 0.32‖		37.2	0.53 ± 0.05

* Unpaired two-tailed *t* test; 19 degrees of freedom.
‡ Unpaired two-tailed *t* test; 32 degrees of freedom.
§ Significantly different as revealed by an unpaired two-tailed *t* test: $p < 0.001$, 19 degrees of freedom. This difference thus reflects the two populations of coated vesicles formed at the plasma membrane and the TGN (14).
‖ Significantly different as revealed by an unpaired two-tailed *t* test: $P < 0.001$, 31 degrees of freedom.
** These values are not statistically significantly different from one another: $P > 0.1$; unpaired two-tailed *t* tests with 51–76 degrees of freedom.

Published April 1, 1993

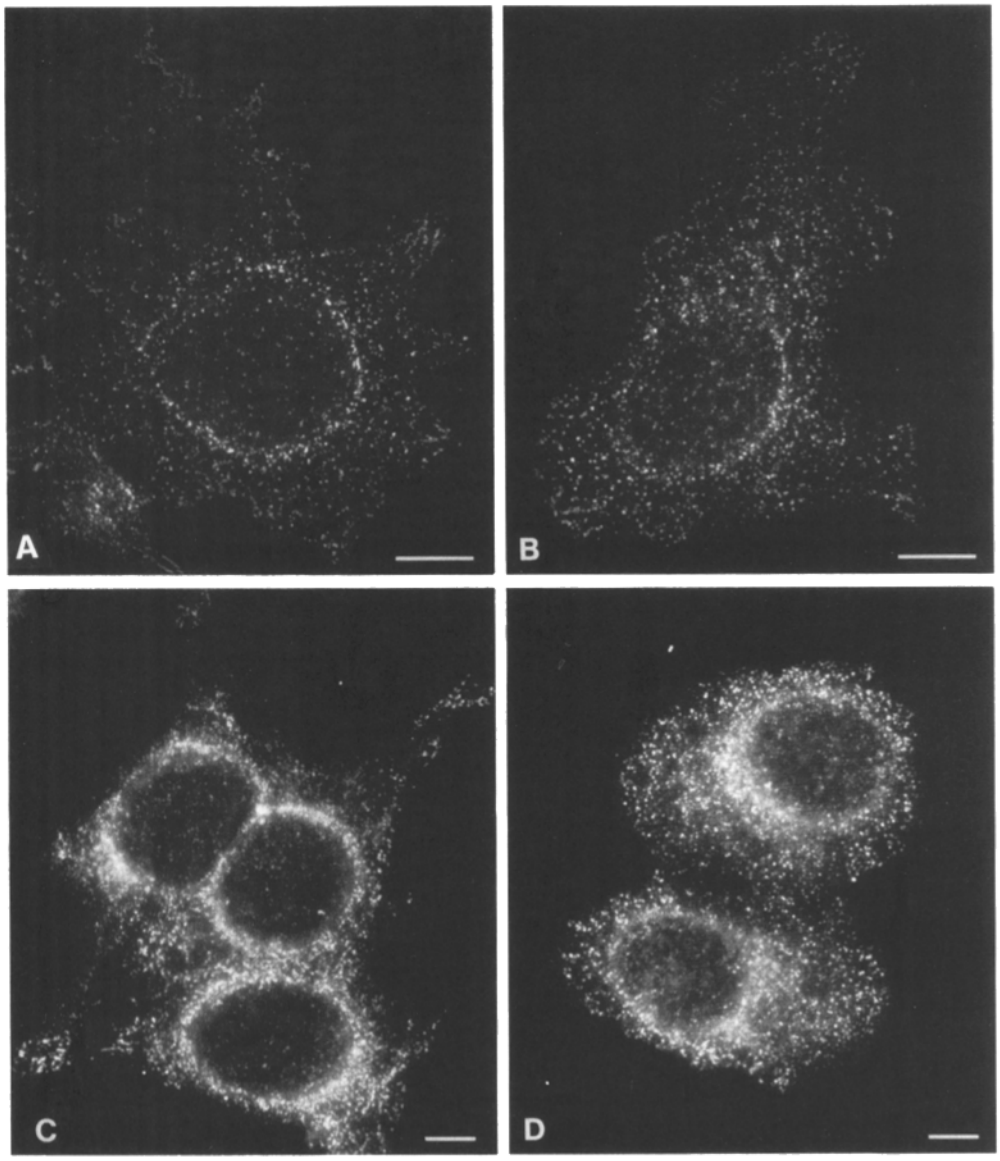

Figure 7. Immunofluorescence microscopy using AP-6 (*A* and *B*) and ACl-M11 (*C* and *D*) followed by first rhodamine-labeled goat anti-mouse IgG and next rhodamine-labeled mouse anti-goat IgG to reveal the distribution of α-adaptins in control (*A*), K^+-depleted (*B* and *C*), and hypertonically treated cells (*D*). Except for the perinuclear area containing Golgi elements, a similar result is obtained with mAb 100/1 specific for the β- and β'-adaptins. Thus the HA2 adaptor occurs in punctate aggregates under all experimental conditions studied. Bar, 10 μm.

Reconstitution Experiments

With the experimental conditions under which clathrin lattices were removed whereas the HA2 adaptors still aggregated in living cells (Fig. 9), it was of interest to see whether clathrin lattices and functional coated pits/vesicles could be reconstituted. When the K^+-free or hypertonic medium was replaced by isotonic K^+-supplemented medium (DME), internalization of transferrin returned to normal as assessed by fluorescence microscopy (data not shown) and biochemical measurements (Fig. 3). The biochemical experiments further revealed that the reconstitution was a gradual process completed only after 30 min in K^+-depleted cells, whereas full reconstitution was not obtained in hypertonically treated cells within the time frame studied. As shown in Fig. 9, after full reconstitution, distinct clathrin lattices with the characteristic punctual pattern matching HA2 adaptor aggregates on the inner aspect of the plasma membrane had reformed in virtually all cells to an extent that was indistinguishable from controls. The matching of immunofluorescence double labeling for clathrin and HA2 adaptors was performed on the flattened, marginal processes and other peripheral parts of the cells. Clearly, matching was not possible in the cytoplasm-rich perinuclear portions, which in addition to clathrin lattices at the cell surface also contain clathrin associated with the TGN as well as the bulk of soluble clathrin. As might be expected from the biochemical data, at earlier time points investigated—1, 2, 5, and 15 min of reconstitution—far more complex results were obtained. After 1 and 2 min of reconstitution, it was possible to match clathrin lattices and HA2 adaptor aggregates in a minor fraction of the cells. This fraction gradually increased with time. Thus the biochemical data (Fig. 3) seem to reflect intercellular heterogeneity in time required for cells to resume endocytosis from coated pits.

Discussion

In this study we have used immunofluorescence and ultrastructural immunogold microscopy combined with biochemical measurements to show in living cells that (*a*) when

Published April 1, 1993

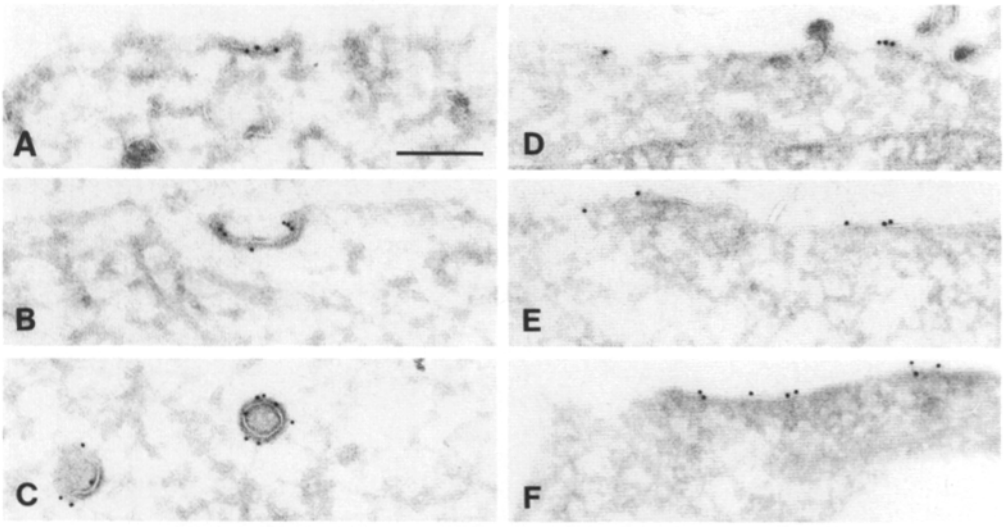

Figure 8. Localization of α-adaptins in cryosections of control (*A–C*), K^+-depleted (*D*) and hypertonically treated (*E* and *F*) HEp-2 cells labeled with anti-α-adaptin antibody AP-6 followed by goat anti-mouse IgG coupled to 10 nm colloidal gold. The figure illustrates the reactivity of AP-6 with flat coated membrane domains (*A*), coated pits (*B*), and coated vesicular profiles (*C*) in control cells. After the removal of coated pits by K^+ depletion (*D*) or incubation in hypertonic medium (*E* and *F*), AP-6 still labels flat plasma membrane domains. It should be noted that the figure (especially *B*, *C*, and *F*) is not representative of the density of labeling obtained with AP-6, which typically was much lower. Bar, 200 nm.

endocytosis of transferrin in HEp-2 cells is arrested by K^+ depletion as well as by incubation in hypertonic medium, intact HA2 adaptor aggregates are still associated with the cytoplasmic face of the plasma membrane whereas membrane-associated clathrin lattices are removed, resulting in accumulation of clathrin in the cytoplasm; and (*b*) acidification of the cytosol reduces size/surface area but increases heterogeneity of clathrin-coated domains of the plasma membrane and TGN. These findings indicate that K^+ depletion and incubation in hypertonic medium interferes with the interaction between clathrin and adaptors whereas cytosol acidification prevents invaginated clathrin-coated domains from pinching off.

Fate of Clathrin

Using immunogold technique on ultrathin cryosections of K^+-depleted and hypertonically treated cells, it is surprising that we do not detect plasma membrane associated clathrin lattices, since this is contradictory to the previous findings of Heuser and Anderson (20). Based on studies of replicas of freeze-etched fibroblast membranes, they found that these experimental treatments result in accumulations of plasma membrane–associated microcages that are empty, that is, devoid of internal membrane. One possible cause for the differing results could be that anti-clathrin C_{HC} 5.9 cannot recognize clathrin in microcages. We consider this possibility rather unlikely, since the antibody efficiently detects clathrins in the soluble and membrane-bound state (5, 18) (this study). As an alternative explanation, we would suggest that both K^+ depletion and incubation in hypertonic medium remove clathrin lattices from membranes and result in formation of clathrin microcages in the cytoplasm, and that at some stage in the preparation of freeze-etched specimens, cytoplasmic clathrin microcages adhere to the inner surface of the plasma membrane. This suggestion is compatible with all the available data. Thus, it explains why membrane-associated clathrin lattices are not detected in K^+-depleted and hypertonically treated cells in routine EM specimens. Furthermore, the presence of microcages within different levels of the cytoplasm would indeed lead to the reported fuzzy granular immunofluorescence specific for clathrin (19, 24) (and this study), since no single level of focus exists, which would appear to be the case if microcages were attached to the plasma membrane. It is also possible that different cell types react differently to these treatments.

This work is to our knowledge also the first to report on the immunocytochemical localization of clathrin in intact cells at the ultrastructural level following acidification of the cytosol. Our results are consistent with the view that this experimental condition prevents formation of coated vesicles from coated pits, by "paralyzing" the pits (19, 44). It furthermore seems that cytosol acidification retards budding of coated vesicles from the TGN (8). Thus acidification of the cytosol may in general paralyze membrane-bound clathrin lattices, thereby preventing budding of coated vesicles.

Our results are thus consistent with the conclusion that K^+ depletion and incubation in hypertonic medium perturb formation of clathrin-coated vesicles by a mechanism different from that of cytosol acidification. Furthermore, using fluorescence photobleaching to study the interaction between mutant influenza virus hemagglutinin HA-Tyr 543 and clathrin-coated pits, Fire et al. (13) showed that whereas incubation in hypertonic medium had no effect on the mobile fraction of HA-Tyr 543, it was significantly reduced by cytosol acidification, indicating that a fraction of HA-Tyr 543 in acidified cells is trapped in paralysed coated pits. There are thus structural as well as functional data to substantiate the conclusion.

Fate of Adaptors

In K^+-depleted as well as hypertonically treated HEp-2 cells where membrane-associated clathrin lattices are removed, intact HA2 adaptor aggregates are still found at the plasma membrane to the same extent as in controls. We con-

Published April 1, 1993

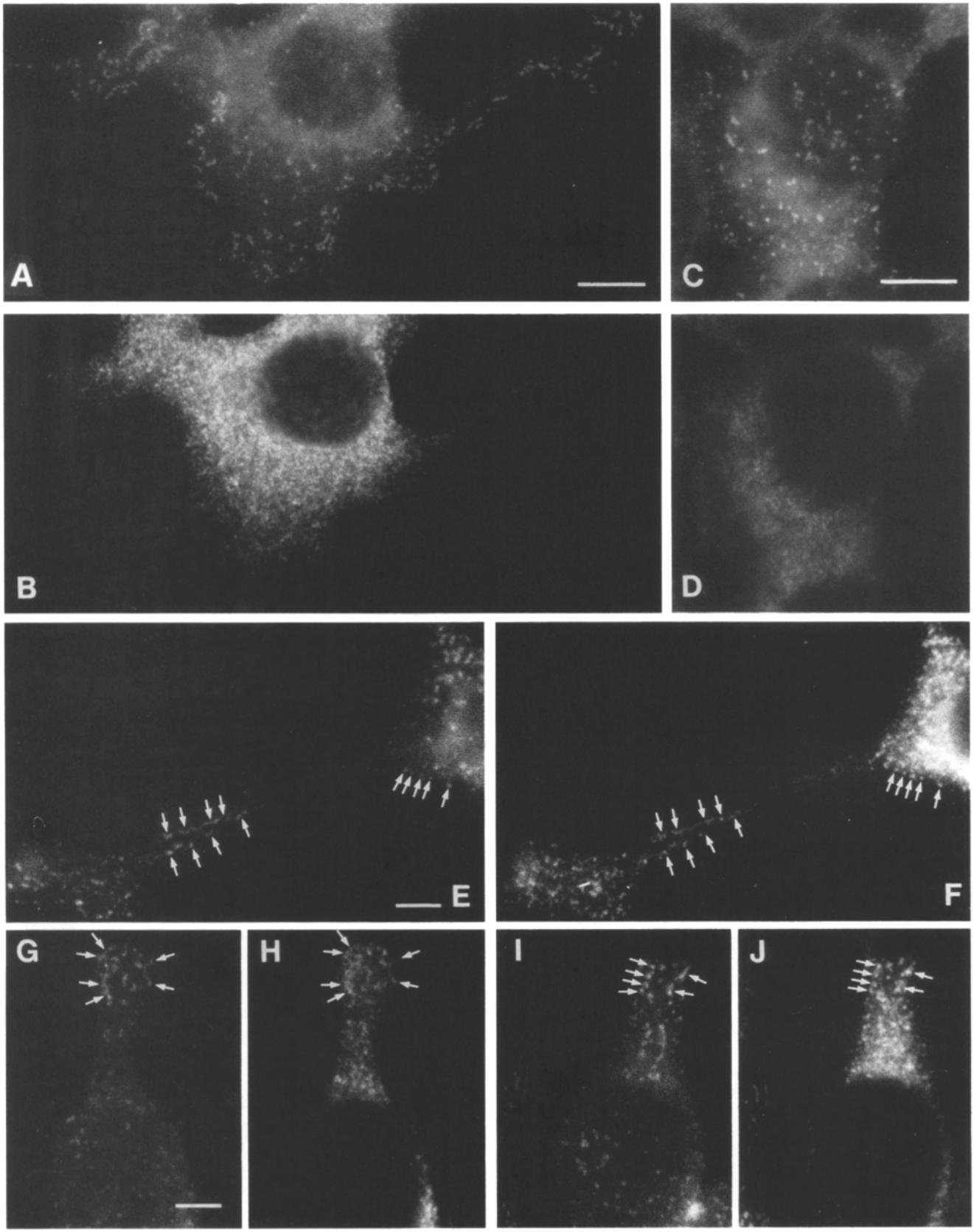

Figure 9. Double-labeling immunofluorescence microscopy of K^+-depleted (*A–D*) and reconstituted (*E–J*) HEp-2 cells using Texas red– and fluorescein-conjugated secondary antibodies to visualize bound anti-α-adaptin (AC1-M11) and anti-clathrin (CHC 5.9), respectively. (*A*, *C*, *E*, *G*, and *I*) Texas red filter to detect HA2 adaptors. (*B*, *D*, *F*, *H*, and *J*) fluorescein filter to detect clathrin. Focus is maintained close to the substratum in all figures except in *C* and *D* where focus is at the cell surface (similar to Fig. 2, *A* and *A'*). Note that in K^+-depleted cells—similar to hypertonically treated cells—the fluorescence specific for α-adaptins is distinctly punctate whereas the fluorescence specific for clathrin is fuzzy granular. After the reconstitution HA2 adaptors and clathrin colocalize–similar to controls—in characteristic patterns as indicated by labeled arrows. Bars: (*A–D*) 10 μm; (*E–J*) 5 μm.

Published April 1, 1993

sider this finding interesting, especially since it is possible—after replacement with isotonic K^+-supplemented medium—to reconstitute clathrin lattices at plasma membrane domains where HA2 adaptors are aggregated and thus form coated pits which generate functional coated vesicles delivering transferrin to endosomes. In this study, we cannot determine if the HA2 adaptor aggregates at the plasma membrane in K^+-depleted and hypertonically treated HEp-2 cells after reconstitution actually nucleate clathrin lattices, or whether "new" HA2 adaptors are recruited together with clathrin from the cytosol. However, our findings do raise the possibility that during reconstitution clathrin lattices are formed at the plasma membrane using pre-existing adaptor aggregates as scaffolding.

Studies by Anderson and co-workers on coated pit formation in vitro are in agreement with the possibility that adaptor aggregates can nucleate clathrin lattices. Plasma membranes from fibroblasts were isolated and attached to a substratum, and clathrin-coated pits were removed by treatment with high pH buffers (32). Subsequently new clathrin-coated pits were generated by incubating the isolated membranes with extracted coat protein. New coated pits assembled at a limited number of specialized regions on the inner aspect of the plasma membrane which in replicas could be identified as patches of aggregated particles (29). Further studies showed that when the plasma membrane of the fibroblasts was labeled with anti-LDL receptor IgG–gold complexes at 4°C, the reconstitution of coated pits at the inner aspect of the isolated plasma membranes resulted in "internalization" of the gold conjugates with a simultaneous loss of clathrin triskelions and HA2 adaptors, indicating that the reconstituted coated pits were capable of coated vesicle formation (27). Although a biochemical or immunochemical characterization of the particle aggregates at which coated pit formation was reported to take place has so far not been performed, it seems likely that they could be composed of HA2 adaptor complexes in addition to integral membrane proteins (29, 30).

It has recently been shown that AP-2 (~HA2) exhibits self association in solution (3) and that this process is highly dependent on the experimental conditions. Based on the data obtained in intact cells and in vitro, it is thus tempting to speculate that adaptors aggregate by self-association and that these adaptor aggregates nucleate clathrin lattices leading to formation of coated pits. The self-association process could be influenced by binding of adaptors to recognition sequences in the cytoplasmic tail of molecules internalized efficiently by coated pits.

We are very grateful to Dr. Margaret S. Robinson, University of Cambridge, UK, for the gift of AC1-M11 antibody, and for critically reading the manuscript. We are also grateful to Dr. Ernst Ungewickell and Dr. Frances Brodsky for the kind gift of mAb 100/1 and AP-6, respectively. We furthermore thank Jorunn Jacobsen, Marianne Lund, Anne-Grethe Myrann, Mette Ohlsen, Keld Ottosen, and Kirsten Pedersen for excellent technical assistance.

This work was supported by grants from the Danish Medical Research Council, the Novo Nordic Foundation, the Danish and Norwegian Cancer Societies, the P. Carl Petersen Foundation, the Marshall Foundation, Nyegaards Foundation, Ib Henriksens Foundation, the Carlsberg Foundation, and by a NATO Collaborative Research Grant (CRG 900517).

Received for publication 14 August 1992 and in revised form 22 December 1992.

References

1. Ahle, S., A. Mann, U. Eichelsbacher, and E. Ungewickell. 1988. Structural relationships between clathrin assembly proteins from the Golgi and the plasma membrane. *EMBO (Eur. Mol. Biol. Organ.) J.* 7:919–929.
2. Backer, J. M., S. E. Shoelson, E. Haring, and M. F. White. 1991. Insulin receptors internalize by a rapid, saturable pathway requiring receptor autophosphorylation and an intact juxtamembrane region. *J. Cell Biol.* 115:1535–1545.
3. Beck, K. A., and J. A. Keen. 1991. Self-association of the plasma membrane-associated clathrin assembly protein AP-2. *J. Biol. Chem.* 266:4437–4441.
4. Brodsky, F. M. 1988. Living with clathrin: its role in intracellular membrane traffic. *Science (Wash. DC).* 242:1396–1402.
5. Bruder, G., and B. Weidenmann. 1986. Identification of a distinct 9S form of soluble clathrin in cultured cells and tissues. *Exp. Cell Res.* 164: 449–462.
6. Chin, D. J., R. M. Straubinger, S. Acton, I. Näthke, and F. M. Brodsky. 1989. 100-kDa polypeptides in peripheral clathrin-coated vesicles are required for receptor-mediated endocytosis. *Proc. Natl. Acad. Sci. USA.* 86:9289–9293.
7. Ciechanover, A., A. L. Schwartz, A. Dautry-Varsat, and H. F. Lodish. 1983. Kinetics of internalization and recycling of transferrin and the transferrin receptor in a human hepatoma cell line. *J. Biol. Chem.* 258:9681–9689.
8. Cosson, P., I. de Curtis, J. Pouyssegur, G. Griffiths, and J. Davoust. 1989. Low cytoplasmic pH inhibits endocytosis and transport from the trans-Golgi network to the cell surface. *J. Cell Biol.* 108:377–387.
9. Daukas, G., and S. H. Zigmond. 1985. Inhibition of receptor-mediated but not fluid-phase endocytosis in polymorphonuclear leukocytes. *J. Cell Biol.* 101:1673–1679.
10. Dautry-Varsat, A., A. Ciechanover, and H. F. Lodish. 1983. pH and the recycling of transferrin during receptor-mediated endocytosis. *Proc. Natl. Acad. Sci. USA.* 80:2258–2262.
11. Davoust, J., J. Gruenberg, and K. E. Howell. 1987. Two threshold values of low pH block endocytosis at different stages. *EMBO (Eur. Mol. Biol. Organ.) J.* 6:3601–3609.
12. Docherty, P. A., and M. D. Snider. 1991. Effects of hypertonic and sodium-free medium on transport of a membrane glycoprotein along the secretory pathway in cultured mammalian cells. *J. Cell Physiol.* 146: 34–42.
13. Fire, E., D. E. Zwart, M. G. Roth, and Y. I. Henis. 1991. Evidence from lateral mobility studies for dynamic interactions of a mutant influenza hemagglutinin with coated pits. *J. Cell Biol.* 115:1585–1594.
14. Friend, D. F., and M. G. Farquhar. 1967. Functions of coated vesicles during protein absorption in the rat vas deferens. *J. Cell Biol.* 35:357–376.
15. Fuhrer, C., I. Geffen, and M. Spiess. 1991. Endocytosis of the ASGP receptor H1 is reduced by mutation of tyrosine-5 but still occurs via coated pits. *J. Cell Biol.* 114:423–431.
16. Griffiths, G., A. McDowell, R. Back, and J. Dubochet. 1983. On the preparation of cryosections for immunocytochemistry. *J. Ultrastruct. Res.* 89:65–78.
17. Hansen, S. H., K. Sandvig, and B. van Deurs. 1991. The preendosomal compartment comprises distinct coated and noncoated endocytic vesicle populations. *J. Cell Biol.* 113:731–741.
18. Hansen, S. H., K. Sandvig, and B. van Deurs. 1992. Internalization efficiency of the transferrin receptor. *Exp. Cell Res.* 199:19–28.
19. Heuser, J. 1989. Effects of cytoplasmic acidification on clathrin lattice morphology. *J. Cell Biol.* 108:401–411.
20. Heuser, J. E., and R. G. W. Anderson. 1989. Hypertonic media inhibit receptor-mediated endocytosis by blocking clathrin-coated pit formation. *J. Cell Biol.* 108:389–400.
21. Hille, A., J. Klumperman, H. J. Geuze, C. Peters, F. M. Brodsky, and K. v. Figura. 1992. Lysosomal acid phosphatase in internalized via clathrin-coated pits. *Eur. J. Cell Biol.* 59:106–115.
22. Ilondo, M. M., P. J. Courtoy, D. Geiger, J. L. Carpentier, G. G. Rousseau, and P. D. Meyts. 1986. Intracellular potassium depletion in IM-9 lymphocytes suppresses the slowly dissociating component of human growth hormone binding and the down-regulation of its receptors but does not affect insulin receptors. *Proc. Natl. Acad. Sci. USA.* 83: 6460–6464.
23. Keen, J. H. 1990. Clathrin and associated assembly and disassembly proteins. *Annu. Rev. Biochem.* 59:415–438.
24. Larkin, J. M., M. S. Brown, J. L. Goldstein, and R. G. W. Anderson. 1983. Depletion of intracellular potassium arrests coated pit formation and receptor-mediated endocytosis in fibroblasts. *Cell.* 33:273–285.
25. Larkin, J. M., W. C. Donzell, and R. G. W. Anderson. 1985. Modulation of intracellular potassium and ATP: effects on coated pit function in fibroblasts and hepatocytes. *J. Cell Physiol.* 124:372–378.
26. Larkin, J. M., W. C. Donzell, and R. G. W. Anderson. 1986. Potassium-dependent assembly of coated pits: new coated pits form as planar clathrin lattices. *J. Cell Biol.* 103:2619–2627.
27. Lin, H. C., M. S. Moore, D. A. Sanan, and R. G. W. Anderson. 1991. Reconstitution of clathrin-coated pit budding from plasma membranes. *J. Cell Biol.* 114:881–891.
28. Madshus, I. H., K. Sandvig, S. Olsnes, and B. van Deurs. 1987. Effect of reduced endocytosis induced by hypotonic shock and potassium depletion

on the infection of Hep 2 cells by picornaviruses. *J. Cell Physiol.* 131:14–22.
29. Mahaffey, D. T., M. S. Moore, F. M. Brodsky, and R. G. W. Anderson. 1989. Coat proteins isolated from clathrin coated vesicles can assemble into coated pits. *J. Cell Biol.* 108:1615–1624.
30. Mahaffey, D. T., J. S. Peeler, F. M. Brodsky, and R. G. W. Anderson. 1990. Clathrin-coated pits contain an integral membrane protein that binds the AP-2 subunit with high affinity. *J. Biol. Chem.* 265:16514–16520.
31. McGraw, T. E., B. Pytowski, J. Arzt, and C. Ferrone. 1991. Mutagenesis of the human transferrin receptor: two cytoplasmic phenylalanines are required for efficient internalization and a second-site mutation is capable of reverting an internalization-defective phenotype. *J. Cell Biol.* 112: 853–861.
32. Moore, M. S., D. T. Mahaffey, F. M. Brodsky, and R. G. W. Anderson. 1987. Assembly of clathrin-coated pits onto purified plasma membranes. *Science (Wash. DC).* 236:558–563.
33. Morris, S. A., S. Ahle, and E. Ungewickell. 1989. Clathrin-coated vesicles. *Curr. Opin. Cell Biol.* 1:684–690.
34. Moya, M., A. Dautry-Varsat, B. Goud, D. Louvard, and P. Boquet. 1985. Inhibition of coated pit formation in Hep-2 cells blocks the cytotoxicity of diphtheria toxin but not that of ricin toxin. *J. Cell Biol.* 101:548–559.
35. Oka, J. N., and P. H. Weigel. 1989. The pathways for fluid phase and receptor mediated endocytosis in rat hepatocytes are different but thermodynamically equivalent. *Biochem. Biophys. Res. Commun.* 159: 488–494.
36. Oka, J. A., M. D. Christensen, and P. H. Weigel. 1989. Hyperosmolarity inhibits galactosyl receptor-mediated but not fluid phase endocytosis in isolated rat hepatocytes. *J. Biol. Chem.* 264:12016–12024.
37. Pearse, B. M. F., and M. S. Robinson. 1990. Clathrin, adaptors, and sorting. *Annu. Rev. Cell Biol.* 6:151–171.
38. Petersen, O. W., and B. van Deurs. 1983. Serial-section analysis of coated pits and vesicles involved in adsorptive pinocytosis in cultured fibroblasts. *J. Cell Biol.* 96:277–281.
39. Robinson, M. S. 1987. 100-kD coated vesicle proteins: molecular heterogeneity and intracellular distribution studied with monoclonal antibodies. *J. Cell Biol.* 104:877–895.
40. Robinson, M. S. 1992. Adaptins. *Trends Cell Biol.* 2:293–297.
41. Sandvig, K., S. Olsnes, J. E. Brown, O. W. Petersen, and B. van Deurs. 1989. Endocytosis from coated pits of Shiga toxin: A glycolipid-binding protein from Shigella dysenteriae. *J. Cell Biol.* 108:1331–1343.
42. Sandvig, K., and B. van Deurs. 1990. Selective modulation of the endocytic uptake of ricin and fluid phase markers without alteration in transferrin endocytosis. *J. Biol. Chem.* 265:6382–6388.
43. Sandvig, K., A. Sundan, and S. Olsnes. 1985. Effect of potassium depletion of cells on their sensitivity to diphtheria toxin and pseudomonas toxin. *J. Cell Physiol.* 124:54–60.
44. Sandvig, K., S. Olsnes, O. W. Petersen, and B. van Deurs. 1987. Acidification of the cytosol inhibits endocytosis from coated pits. *J. Cell Biol.* 105:679–689.
45. Schmid, S. L. 1992. The mechanism of receptor-mediated endocytosis: More questions than answers. *BioEssays.* 14:589–596.
46. Slot, J. W., H. J. Geuze, and A. H. Weerkamp. 1988. Localization of macromolecular components by application of the immunogold technique on cryosectioned bacteria. *Methods Microbiol.* 20:211–236.
47. Slot, J. W., G. Posthuma, L.-Y. Chang, J. D. Crapo, and H. J. Geuze. 1989. Quantitative aspects of immunogold labeling in embedded and nonembedded sections. *Am. J. Anat.* 185:271–281.
48. Stoppelli, M. P., C. Tacchetti, M. V. Cubellis, A. Corti, V. J. Hearing, G. Cassani, E. Appella, and F. Blasi. 1986. Autocrine saturation of prourokinase receptors on human A431 cells. *Cell.* 45:675–684.
49. Tokuyasu, K. T. 1980. Immunocytochemistry on ultrathin cryosections. *Histochem. J.* 12:381–403.
50. Tokuyasu, K. T. 1989. Use of poly(vinylpyrrolidine) and poly(vinylalcohol) for cryoultramicrotomy. *Histochem. J.* 21:163–171.
51. Trowbridge, I. S. 1991. Endocytosis and signals for internalization. *Curr. Opin. Cell Biol.* 3:634–641.
52. van Deurs, B., O. W. Petersen, S. Olsnes, and K. Sandvig. 1989. The ways of endocytosis. *Int. Rev. Cytol.* 117:131–177.
53. Vaux, D. 1992. The structure of an endocytosis signal. *Trends Cell Biol.* 2:189–192.
54. Weibel, E. R. 1979. Stereological Methods. Vol. 1. Practical Methods for Biological Morphometry. Academic Press, London.
55. West, M. A., M. S. Bretscher, and C. Watts. 1989. Distinct endocytotic pathways in epidermal growth factor-stimulated human carcinoma A431 cells. *J. Cell Biol.* 109:2731–2739.
56. Wiedlocha, A., K. Sandvig, H. Walzel, C. Radzikowsky, and S. Olsnes. 1991. Internalization and action of an immunotoxin containing mistletoe lectin A-chain. *Cancer Res.* 51:916–920.